

A two-surface anisotropic damage/plasticity model for plain concrete

E.Hansen & K.Willam

University of Colorado Boulder, Boulder Colorado, USA

I.Carol

ETSECCPB-UPC, Barcelona, Spain

ABSTRACT: Concrete is a material whose performance is governed by the subtle interaction of its cohesive and frictional constituents. Since the theories of plasticity, damage mechanics, and fracture mechanics cannot, by themselves, capture both of these phenomena, a novel constitutive model is proposed which combines the theories of plasticity and damage mechanics in a multi-surface formulation. Synthesis of these two constitutive concepts describes not only the hardening/softening behavior of concrete under compressive loading, but also the decrease of material strength and stiffness under tension. The characteristics and behavior of the concrete model are presented through performance studies of specimens under monotonic and cyclic loading in tension, compression, and shear.

1 INTRODUCTION

The objective of this paper is to present a novel constitutive concept for concrete, that merges the advantages of damage mechanics and plasticity into one formulation. Concrete loaded in tension experiences the formation of microcracks due to loss of cohesion between the concrete aggregate and matrix. This decohesion results in a reduction of both strength and stiffness on the macroscopic material level. Damage mechanics captures not only loss of material strength, but also deterioration of the material stiffness. On the other hand, concrete loaded in compression is much more ductile than in tension. The inelastic hardening response up to peak is followed by a ductile softening response if the confining pressures are low. Under high confinement the initial elastic material stiffness degrades only little in the pre-peak response regime. Thus plasticity provides a natural formulation to capture the degradation of frictional strength of concrete and the so-called Reynolds effect, the dilatant behavior of materials when subjected to shear.

The proposed constitutive model uses a two-surface damage/plasticity formulation to capture these very different responses under tension and compression. The damage formulation is a Rankine-type anisotropic damage model, based on the Pseudo-Rankine anisotropic damage model of Carol et al. (2001). The plasticity formulation is a parabolic extension of the classic two-invariant model of Drucker and Prager (Drucker and Prager 1952). To allow for interaction between the two inelastic processes, both models are formulated in terms of the effective stress and strain in damage space. Since it is assumed that the material stiffness degrades due to tensile loading only, stiffness recovery/degradation is controlled

through the use of projection operators which modify the damage tensor. At the intersection of the damage and plasticity surfaces the solution is attained by enforcing consistency for both surfaces in order to determine which surface(s) is (are) activated by the current loading condition.

2 INDEPENDENT DAMAGE AND PLASTICITY FORMULATIONS

2.1 Anisotropic damage model of Rankine-type

For the description of elastic degradation a Rankine-type anisotropic damage model is adopted, which has been recently proposed in Carol et al. (2001). It uses second-order damage tensors to express direction-dependent material damage. The damage tensors are used to define the relation between the externally measured nominal stress and strain and the effective stress and strain inside the region of microcracking. The onset and progression of material degradation is based upon the strain energy associated with the effective stress and strain. The essential aspects of the model are summarized in the following section.

2.1.1 Nominal/effective stress-strain relations

Material degradation may be thought of as the average effect of distributed microcracking. Effective stresses and effective strains are those experienced by the material skeleton between microcracks. In contrast, stresses and strains observed externally are the nominal stresses and strains. The relations between nominal and effective stress and strain are established by the damage variables and their evolution laws.

In this formulation, anisotropic damage is represented by a second-order damage tensor. This can be

for example the traditional damage tensor D_{ij} which varies from 0 to δ_{ij} or, more conveniently, the integrity tensor $\bar{\phi}_{ij}$ ($\bar{\phi}_{ij} = \delta_{ij} - D_{ij}$), varying from δ_{ij} to zero, or its inverse ϕ_{ij} , varying from δ_{ij} to ∞ .

Product-type symmetrization is applied to insure symmetry of the nominal and effective stress and strain tensors, resulting in

$$\sigma_{ij} = \bar{w}_{ik} \sigma_{kl}^{\text{eff}} \bar{w}_{lj} \quad (1)$$

where \bar{w}_{ik} is the square root of the integrity tensor. If equivalence of the strain energy in terms of nominal and effective stress/strain is assumed ($W = W^{\text{eff}}$, $W = 1/2 \sigma : \epsilon$), the effective/nominal strain relation takes the dual form

$$\epsilon_{ij}^{\text{eff}} = \bar{w}_{ik} \epsilon_{kl} \bar{w}_{lj} \quad (2)$$

These relations and their inverses may be rewritten in a more convenient manner introducing the fourth order 'damage-effect tensor' $\bar{\alpha}_{ijkl}$:

$$\bar{\alpha}_{ijkl} = \frac{1}{2} (\bar{w}_{ik} \bar{w}_{jl} + \bar{w}_{il} \bar{w}_{jk}) \quad (3)$$

$$\sigma_{ij} = \bar{\alpha}_{ijkl} \sigma_{kl}^{\text{eff}} \quad ; \quad \epsilon_{ij}^{\text{eff}} = \bar{\alpha}_{ijkl} \epsilon_{kl} \quad (4)$$

$$\sigma_{ij}^{\text{eff}} = \alpha_{ijkl} \sigma_{kl} \quad ; \quad \epsilon_{ij} = \alpha_{ijkl} \epsilon_{kl}^{\text{eff}} \quad (5)$$

where α_{ijkl} is the inverse of $\bar{\alpha}_{ijkl}$. Additionally, the damage-effect tensor $\bar{\alpha}_{ijkl}$ and its inverse may be extended to obtain expressions for the secant stiffness and secant compliance. For simplicity, it is assumed that the effective stress-strain relations are linear elastic, i.e.

$$\sigma_{ij}^{\text{eff}} = E_{ijkl}^0 \epsilon_{kl}^{\text{eff}} \quad ; \quad \epsilon_{ij}^{\text{eff}} = C_{ijkl}^0 \sigma_{kl}^{\text{eff}} \quad (6)$$

Combining these relations with those of Eqs. 4 and 5 leads to the secant relations for the nominal stresses and strains:

$$E_{ijkl} = \bar{\alpha}_{ijpq} E_{pqrs}^0 \bar{\alpha}_{klrs}; C_{ijkl} = \alpha_{pqij} C_{pqrs}^0 \alpha_{rskl} \quad (7)$$

Substituting Eqns.3–5 into Eqn.7 and simplifying the equations, one finally obtains the same expression of secant stiffness as proposed in (Valanis 1990).

2.1.2 Loading function and strain evolution

To insure consistency between the damage and plasticity formulations, damage is formulated in the spirit of plasticity. The total strain increment is thus decomposed into elastic and degrading strain components, $\dot{\epsilon} = \dot{\epsilon}_e + \dot{\epsilon}_d$. The boundary between the regions of elastic behavior and progressive damage is governed by the damage condition, $F_d = F_d(\sigma, \mathbf{q}_d) = 0$, where \mathbf{q}_d are the damage history variables which describe the evolution of the damage surface. The damage rule and the consistency condition may be derived in a manner similar to elastoplasticity, such that $\dot{\epsilon}_d = \dot{\lambda}_d \mathbf{m}_d$ and $\dot{F}_d = \mathbf{n}_d : \dot{\sigma} - H_d \dot{\lambda}_d = 0$ (Carol, Rizzi, and Willam 1994).

The associated loading function for the Rankine-type anisotropic damage model is defined in terms of modified (principal tensile) conjugate forces \hat{y} as

$$F_d = \max(-\hat{y}_{(1)}, -\hat{y}_{(2)}, -\hat{y}_{(3)}) - r(L) \quad (8)$$

Note that the initial damage surface in conjugate force space follows the maximum stress hypothesis of Rankine. The conjugate force $-y_{ij}$ of this formulation is a second order energy tensor:

$$-y_{ij} = \frac{1}{2} \sigma_{ik}^{\text{eff}} \epsilon_{kj}^{\text{eff}} \quad (9)$$

These forces are the conjugate variables to the 'pseudo-logarithmic' rate of damage defined as $\dot{L}_{ij} = 2\bar{w}_{ik} \dot{\phi}_{kl} \bar{w}_{lj}$. Both, \dot{L}_{ij} , and the conjugate force $-y_{ij}$ exhibit a number of intriguing properties. For instance, the first invariant represents the elastic energy, $-y_{ii} = \frac{1}{2} \sigma_{ik}^{\text{eff}} \epsilon_{ki}^{\text{eff}}$. \dot{L}_{ij} is in general a non-holonomic rate (not an exact differential), while its first invariant has a well defined path-independent integral $L = I_{kk}/3$, which is related to the principal values of the inverse integrity tensor:

$$L = \frac{1}{3} (\ln \phi_{(1)}^2 + \ln \phi_{(2)}^2 + \ln \phi_{(3)}^2) = \frac{2}{3} \ln(\phi_{(1)} \phi_{(2)} \phi_{(3)}) \quad (10)$$

The exponential resistance function $r(L)$ takes the form of the complementary energy,

$$r(L) = r_o e^{-3kL}; \quad r_o = \frac{(f'_t)^2}{2E_o}; \quad k = r_o/g_f \quad (11)$$

Thereby the exponential rate of decay is controlled by L and the Mode I fracture energy per unit volume g_f , i.e. the area under the complete uniaxial stress-strain curve, Fig. 1. The parameter r_o in Eq. 11 and Fig. 1 denotes the elastic strain energy at the peak of the uniaxial tension test. These simple relations may be obtained because the model exhibits closed-form solutions for loading in uniaxial tension. In analogy to plasticity, the evolution of damage strain is defined by $\dot{\epsilon}_d = \dot{\lambda}_d \mathbf{m}_d$, where $\dot{\lambda}_d$ is the damage multiplier and \mathbf{m}_d the evolution direction. A similar argument can be

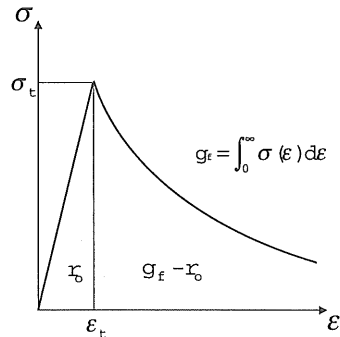


Figure 1: Uniaxial stress-strain curve defining r_o , g_f

made to define the pseudo-log damage rate tensor \dot{L}_{rs} :

$$\dot{L}_{rs} = \dot{\lambda}_d \mathcal{M}_{rs} \quad (12)$$

where \mathcal{M}_{rs} defines the direction of damage evolution. For associated flow, $\mathcal{M}_{rs} = \mathcal{N}_{rs}$, where \mathcal{N}_{rs} is the normal to the damage surface, $\frac{\partial F_d}{\partial (-y_{rs})}$. From Eqn. 12 the inverse integrity tensor ϕ_{pq} can be updated by determining its rate.

$$\dot{\phi}_{pq} = \frac{1}{2} w_{pr} \dot{L}_{rs} w_{sq} \quad (13)$$

where w_{ij} is the square root tensor of the inverse integrity ϕ_{ij} . Once ϕ_{ij} is updated, the rest of the damage tensors as well as the damage-effect tensors can be evaluated, as well as the nominal stress and strain and the secant stiffness and compliance.

2.2 Parabolic Drucker-Prager model

The parabolic Drucker-Prager model is an extension of the classic two-invariant plasticity model (Drucker and Prager 1952).

2.2.1 Yield function

The yield function for the parabolic extension of the Drucker-Prager model takes the form

$$F_p(\sigma) = \alpha I_1 + J_2 - \beta \quad (14)$$

where $I_1 = \sigma_{kk}$ is the first stress invariant and $J_2 = s_{ij}s_{ij}/2$ is the second deviatoric stress invariant ($s_{ij} = \sigma_{ij} - \sigma_{kk}\delta_{ij}/3$). The strength parameters α and β may be expressed in terms of the uniaxial tensile and compressive strengths values of concrete,

$$\alpha = \frac{f'_c - f'_t}{3} \quad ; \quad \beta = \frac{f'_c f'_t}{3} \quad (15)$$

2.2.2 Hardening and softening

The parabolic Drucker-Prager yield surface defined by Eq. 14 expands and contracts isotropically through the use of hardening and softening functions. These functions modify the two strength parameters α and β , changing the material limit point, depending on the magnitude of the plastic strains ϵ_p . The yield function then becomes $F_p(\sigma, \epsilon_p) = \alpha_{hs} I_1 + J_2 - kc\beta$ where k is the hardening parameter, ($k_o < k < 1.0$), c the softening parameter, ($1 \geq c \geq c_o$), and α_{hs} the modified α parameter for hardening/softening, defined by $\alpha_{hs} = kc \frac{1}{3} (f'_c - f'_t)$.

The hardening function adopted for the parabolic Drucker-Prager model was originally outlined by Etse et al. (Etse and Willam 1994) in the context of their three invariant Extended Leon model. It defines the hardening parameter evolution as

$$k(\bar{\epsilon}_p) = \frac{2}{h_D} (1 - k_o) (\sqrt{2h_D \bar{\epsilon}_p} - \bar{\epsilon}_p) + k_o \quad (16)$$

where $\bar{\epsilon}_p$ is the equivalent plastic strain defined by $\bar{\epsilon}_p = \int_t \sqrt{\dot{\epsilon}_p} : \dot{\epsilon}_p dt$ and k_o defines the onset of harden-

ing behavior. Parameter h_D defines the material ductility,

$$h_D = A_h \left(\frac{I_1}{f'_c} \right)^2 + B_h \left(\frac{I_1}{f'_c} \right) + C_h \quad (17)$$

where A_h , B_h , and C_h are constants. Since h_D is dependent upon I_1 , it is able to reflect the effects of confining pressures.

Once the material reaches peak at f'_c , it may begin to soften if the confining pressures are low. In this case the softening function is a Gaussian decay function, defined by

$$c(\bar{\epsilon}_p^t) = \frac{1}{\exp\left(\frac{\xi}{s_D}\right)^2} \quad ; \quad c > c_o \quad (18)$$

Softening under plastic behavior is assumed to be caused by the tensile components of the plastic strain, represented by the equivalent tensile plastic strain, $\bar{\epsilon}_p^t = \int_t \sqrt{\langle \dot{\epsilon}_p \rangle} : \langle \dot{\epsilon}_p \rangle$, where the McCauly brackets $\langle \rangle$ extract only the tensile components of the plastic strains. Furthermore, $\bar{\epsilon}_p^t$ represents the tensile plastic strains which accumulate after the material reaches peak, so $\bar{\epsilon}_p^t = 0$ in the pre-peak regime. ξ in Eq. 18 is a scaling parameter, while s_D is the ductility function for softening, which determines the variation of softening based upon the confinement,

$$s_D = -4.3((\sigma_p - \gamma f'_t)/(\gamma f'_t) + 1.0) + 0.7 \quad (19)$$

where σ_p is the sum of the confining pressures, and where γ is a constant. The constants are chosen such that the material softens completely under unconfined loading and is perfectly plastic under high confinement.

3 TWO-SURFACE ANISOTROPIC DAMAGE/PLASTICITY FORMULATION

3.1 Strain and stress variables

One principal issue of the damage/plasticity combination is which stresses and strains enter the formulation in each part of the model. To this end, the following stresses and strains are defined. First, a decomposition of strain rate in three parts for elastic, degrading and plastic parts is assumed:

$$\dot{\epsilon} = \dot{\epsilon}_e + \dot{\epsilon}_d + \dot{\epsilon}_p \quad (20)$$

Plastic strains are irreversible in nature and can be integrated $\epsilon_p = \int \dot{\epsilon}_p dt$. Then the elastic-damage strain is introduced in the total value, ϵ_{ed} , as:

$$\epsilon_{ed} = \epsilon - \epsilon_p \quad (21)$$

Finally, the effective counterparts of all these strains and stresses are introduced:

$$\sigma_{ij}^{\text{eff}} = \alpha_{ijkl} \sigma_{kl}, \quad \epsilon_{ij}^{\text{eff}} = \bar{\alpha}_{ijkl} \epsilon_{kl} = \epsilon_{ij}^{\text{eff},ed} + \epsilon_{ij}^{\text{eff},p} \quad (22)$$

$$\epsilon_{ij}^{\text{eff},ed} = \bar{\alpha}_{ijkl} \epsilon_{kl}^{\text{ed}}, \quad \epsilon_{ij}^{\text{eff},p} = \bar{\alpha}_{ijkl} \epsilon_{kl}^p \quad (23)$$

3.2 Stiffness recovery

The inverse integrity tensor ϕ_{ij} reflects the current state of damage due to microcracks without distinguishing which microcracks may be open or closed under the current loading state. As suggested by Ortiz (1985), one way of representing stiffness recovery due to microcrack closure consists of defining an 'active' damage tensor, in this case, ϕ_{ij}^{act} , based on the concept of positive and negative projection operators.

The original projection operator concept was introduced in the form of fourth-order tensors. For our purposes, a second-order projection operator for stiffness recovery suffices which is defined as

$$P_{ij}^+ = \sum_{k=1}^3 \mathcal{H}[\epsilon_{ed}^{(k)+}] n_i^{(k)} n_j^{(k)} \quad (24)$$

where $\epsilon_{ed}^{(k)+}$ are the principal tensile components of the elastic-damage strain and n_i are its principal directions.

Using this projection operator, the active inverse integrity tensor is defined as

$$\phi_{ij}^{\text{act}} = \delta_{ij} + P_{ik}^+ \Delta \phi_{kl} P_{lj}^+ \quad ; \quad \Delta \phi_{kl} = \phi_{kl} - \delta_{kl} \quad (25)$$

where ϕ_{kl} is the total inverse integrity tensor. A few basic properties of the active integrity tensor may be identified as

- at initial, undamaged state

$$\phi_{ij}^{\text{act}} = \phi_{ij} = \delta_{ij} \quad (26)$$

- under triaxial tension (damage in all directions)

$$\phi_{ij}^{\text{act}} = \phi_{ij} > \delta_{ij} \quad (27)$$

- under triaxial compression (stiffness recovery in all directions)

$$\phi_{ij}^{\text{act}} = \delta_{ij} \quad (28)$$

3.3 Loading functions for the two-surface model

According to the previous sections, the loading functions for the damage-plasticity model may be expressed as

$$F_d = \max(-\hat{y}_{(1)}^{ed}, -\hat{y}_{(2)}^{ed}, -\hat{y}_{(3)}^{ed}) - r_d(L) \quad (29)$$

$$F_p = \alpha I_1^{\text{eff}} + J_2^{\text{eff}} - r_p(\epsilon_p) \quad (30)$$

where the conjugate forces of the damage surface $-\hat{y}_{(i)}^{ed}$ are defined in terms of the elastic-damage effective strains, and the stress invariants in the plasticity surface in terms of effective stress:

$$-\hat{y}_{ij}^{ed} = \frac{1}{2} \langle \sigma_{ik}^{\text{eff}} \rangle \langle \epsilon_{kj}^{\text{eff}, ed} \rangle \quad (31)$$

$$I_1^{\text{eff}} = \text{tr}(\sigma^{\text{eff}}) \quad ; \quad J_2^{\text{eff}} = \frac{1}{2} \mathbf{s}^{\text{eff}} : \mathbf{s}^{\text{eff}} \quad (32)$$

where $\mathbf{s}^{\text{eff}} = \sigma^{\text{eff}} - 1/3 I_1^{\text{eff}} \mathbf{I}_2$.

Likewise, plastic strains produced by the plastic model are interpreted as effective plastic strains, $\epsilon^{\text{eff}, p}$. In this way, both loading surfaces may be represented in the same space of effective stress, which is convenient and intuitive. At this stage it is assumed that the resistance functions r_d and r_p exhibit no interaction between damage and plasticity. Nevertheless, while the two failure mechanisms are not explicitly coupled, they are implicitly linked by plasticity formulated in effective space and damage dependent upon the elastic/reversible strains (which are based on the plastic strains).

The resulting failure envelope for the two-surface formulation in plane effective stress space is shown in Fig. 2. The bounds of material failure are defined by the inner surfaces, so damage controls in the tension/tension quadrant while plasticity governs the compression/compression quadrant. In the tension/compression regions, the damage model controls the response behavior as far as the intersection of the two surfaces. At this point, both formulations are active, while beyond this point plasticity controls. Note that the surfaces pass through both, the uniaxial tensile strength f_t' and the compressive strength f_c' .

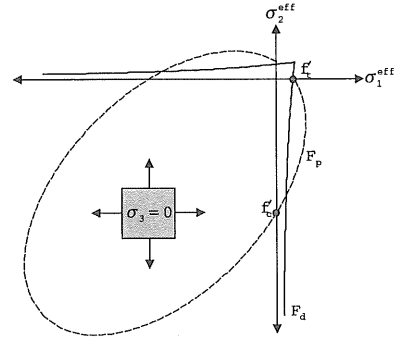


Figure 2: Plane stress envelope for the two-surface model

3.4 Active surface(s) and integration

Plastic integration is performed using the elastic trial-plastic corrector scheme. If the elastic trial only violates one of the two surfaces, standard techniques for one surface are used. If the trial stresses violate both conditions $F_d > 0$ and $F_p > 0$, the program starts the two-surface integration algorithm, the first step of which is to determine the correct set of active surfaces. This may involve two different types of checks.

The first type of check is to ensure whether a 'corner' situation is really reached, since this is not necessarily implied by having both failure functions violated at the trial state of a large increment, especially

if one of the surfaces lies inside the other. A condition as such as this is easily detected by subincrementing the strain step $\Delta\epsilon$ and checking the failure functions at each subincrement.

If subincrementation still shows that a corner situation is reached, a second type of check is applied to find out whether, for the specific strain increment prescribed, the situation is resolved with two surfaces active or only one (i.e. the new one activated, while the one initially active, deactivates). This can only be solved by trial and error, by assuming the set of active surfaces and then verifying whether it was correct, and if not changing the initial assumption and verifying again (Carol and Prat 1995). The verification itself also requires two steps. For each surface assumed active, the consistency condition should hold:

$$\dot{F}_i = \mathbf{n}_i : \dot{\boldsymbol{\sigma}} - H_i \dot{\lambda}_i = 0; \mathbf{n}_i = \frac{\partial F_i}{\partial \boldsymbol{\sigma}}; H_i = -\frac{\partial F_i}{\partial \lambda_i} \quad (33)$$

Solving the linear system (or single equation) implied by this condition leads to the scalar multiplier(s) $\dot{\lambda}_i$ of the surface(s) assumed active. These should be all positive; if not, the assumption was wrong. But even if all turn out positive, a second check is needed. For the surface(s) assumed inactive, we must also verify that $\dot{F}_i \leq 0$. If not, the assumption on the active set was also wrong.

In the case that either the damage or plasticity surface is active, the stress state is returned to the respective surface by a standard return algorithm based on the bisection method. If both surfaces are active, a modified return algorithm is used with applies nested bisection algorithms to return the stress state to the intersection of the damage and plasticity surfaces. Additionally, since the consistency conditions are dependent upon both the normal to the failure surfaces and the plastic/damage flow directions, adopting non-associated flow rules for either damage or plasticity gives greater control over the activation of the failure surfaces. More details on the implementational aspects may be found in (Hansen 2000).

4 PERFORMANCE OF TWO-SURFACE MODEL

4.1 Uniaxial tension

One of the basic principles of the two-surface formulation is that damage controls the material behavior under tensile loading. Thus, when properly calibrated with the fracture energy per unit volume g_f , the model shows active damage in tension (Fig. 3), with good agreement with experimental results. As dictated by damage mechanics, unloading and reloading always occur at the current secant stiffness.

4.2 Uniaxial compression

While damage controls the material behavior under tensile loading, plasticity controls the behavior under compression. With the hardening and softening parameters properly calibrated, the model shows good agreement with experimental results under uncon-

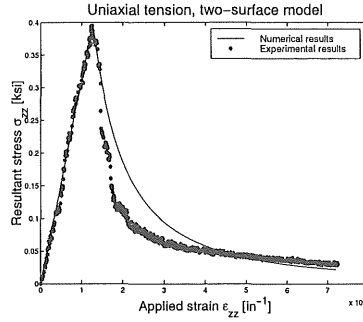


Figure 3: Uniaxial tension, two-surface model

finied uniaxial compression (Fig. 4). Note that under plastic behavior, unloading and reloading occurs elastically. Additionally, the hardening and softening rules are robust enough to capture concrete response under increasing levels of confinement (Fig. 5).

4.3 Cyclic uniaxial tension/compression

It was previously mentioned that the presence of plastic strains have a detrimental effect on the damage response. However, this problem is resolved if damage is expressed in terms of the elastic strains instead of the total strains. This conclusion is tested by cycling

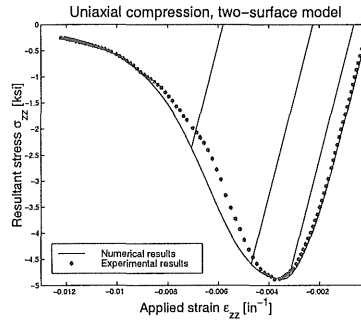


Figure 4: Uniaxial compression, two-surface model, unconfined compression

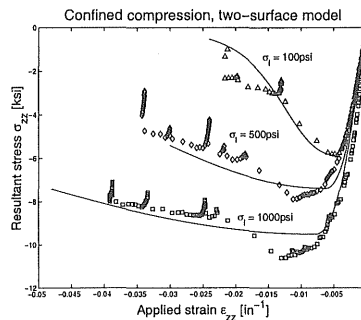


Figure 5: Uniaxial compression, two-surface model, confined compression

a uniaxial tension/compression load, which produces both degrading and plastic strains in the same direction. The results are shown in Fig. 6(a). As shown, damage controls the response under tension, while plasticity is active under compression. While the material unloads at the degraded secant stiffness under tension, the elastic stiffness is recovered when the material compresses, simulating the closing of microcracks. When the material cycles back to tension, the degraded secant stiffness is recovered, simulating the re-opening of the microcracks. Even when plastic strains are present, the material stiffness degrades at the boundary between compression and tension, and material degradation re-commences when the current stress reaches the previous cycle's final stress level (Fig. 6(b)).

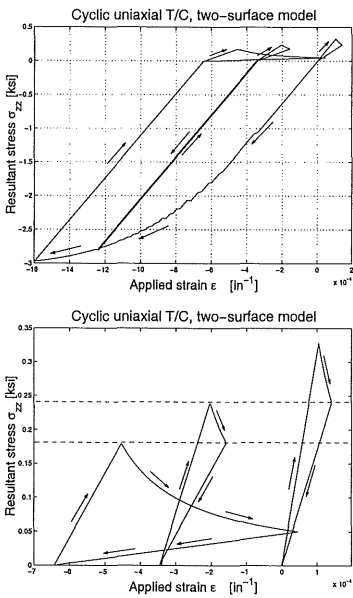


Figure 6: Cyclic uniaxial tension/compression - (a) Total response, (b) Tensile stress close-up

4.4 Equibiaxial tension/compression

The two-surface model is also capable of capturing the effects of active damage and plasticity in two directions. Subjecting the model to equibiaxial tension and compression ($\dot{\epsilon}_{xx} = -\dot{\epsilon}_{yy}$) results in active damage and plasticity in orthogonal directions (Fig. 7). Note that the subsequent analyses assume perfect plasticity in order to detect the fundamental features of the combined damage/plasticity model without the added effects of hardening and softening. Fig. 7(a) shows the response in the direction of tensile loading. As dictated by the two-surface model, damage controls the response in the tensile direction, and so the material loads elastically up to the damage surface, at which point damage commences and the ma-

terial strength degrades. In the compressive direction, the response is governed by plasticity, so the material loads elastically up to the yield surface, at which point perfectly plastic behavior commences. Additional insight into this behavior may be found by observing the stress path in the effective stress space, Fig. 8. The material loads elastically up to the damage surface, at which point damage commences. The stress state then follows the damage surface until it reaches the intersection of the damage and plasticity surfaces. As mentioned, the number of active surfaces depends upon \mathbf{n} and \mathbf{m} for both failure mechanisms, and assuming non-associated flow rules gives a level of control over the surface(s) activation. If a non-associated plastic flow rule is adopted, the stress state can be confined

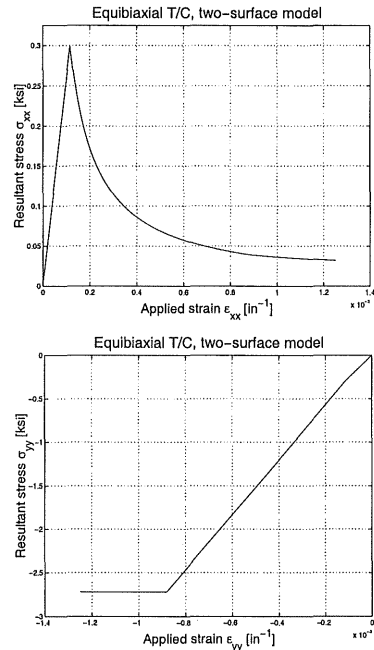


Figure 7: Equibiaxial T/C, two-surface model, non-associated flow - (a) xx-direction, (b) yy-direction

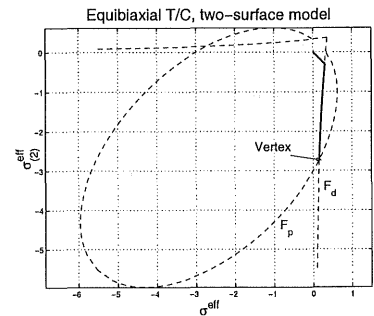


Figure 8: Equibiaxial T/C, non-associated flow - stress path

to the vertex of the damage and plasticity surfaces, shown in Fig. 8. This results in perfect damage in effective space (continuing damage in nominal space) and perfect plasticity in both effective and nominal space. If, instead, associate flow is assumed for both damage and plasticity, the stress path will eventually move away from the vertex and continue along the plasticity surface, resulting in the response of Fig. 9. In this case, the compression continues to increase as

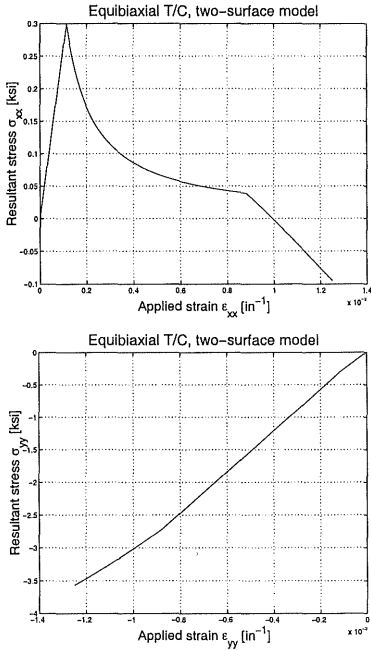


Figure 9: Equibiaxial T/C, two-surface model, associated flow - (a) xx-direction, (b) yy-direction

the stress state follows the plasticity surface. The tensile stress, however, exhibits a change from tension to compression as the stress state moves from the vertex onto the plasticity surface (Fig. 10). While this change in the sign of the stress in the direction of tensile strain seems unnatural at first, a possible explanation can be offered if the dilatancy of the concrete is considered. The dilatancy due to the compressive strains is controlled by the plastic flow rule \mathbf{m}_p and prescribes dilatant strains and stresses orthogonal to the direction of compressive loading. However, the strains orthogonal to the compressive loading are constrained by the rate of tensile loading $\dot{\epsilon}_{xx}$. If the rate of tensile loading is slower than the rate of dilatancy due to the compressive loading, the tensile strain rate $\dot{\epsilon}_{xx}$ serves to constrain the dilatant response, which may result in compressive stresses σ_{xx} . Additional information may be found in (Hansen 2000).

5 CONCLUSIONS

This paper presented a two-surface anisotropic damage/plasticity model which accounts for:

- Damage response under tensile loading, plasticity response under compressive loading.

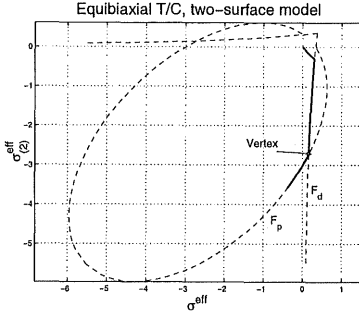


Figure 10: Equibiaxial T/C, associated flow - stress path

- Stiffness recovery when moving from tension to compression to simulate the closing of microcracks.
- Active plasticity and damage where appropriate in the tension/compression regions.

Damage under tension and plasticity under compression is achieved through the use of the Rankine-type anisotropic damage model and the parabolic Drucker-Prager plasticity model. Formulating both models in effective stress/strain space allows interaction between the two surfaces in the same space. Furthermore, damage considers the effects of the elastic strains, which takes into account the effects of the plasticity-induced plastic strains on the damage response. Material stiffness recovery is based on the use of second order projection operators P_{ij}^+ to form the active integrity tensor ϕ_{ij}^{act} , a measure of the current state of material damage at the current load increment. Active damage and plasticity occurs when the effective stress path reaches the intersection of the two surfaces. The two-surface consistency condition is used to determine if one or both of the loading surfaces are indeed active.

The performance of the model was examined by observing the model response under monotonic and cyclic uniaxial tension/compression, and monotonic equibiaxial tension/compression. The monotonic uniaxial tension and compression results show that the model is capable of accurately reproducing the response of concrete under tension and compression. The cyclic uniaxial tension/compression results highlight the stiffness degradation and recovery response of the two-surface model. The equibiaxial tension/compression results show the model response when both surfaces are active, which is directly controlled by the underlying damage and plastic flow rules.

Further work includes investigation into the model behavior at the vertex of damage and plasticity. The behavior at this point is highly dependent upon the flow directions of the two loading mechanisms, which strongly affects the dilatant response. Furthermore, compressive damage needs to be considered. Strictly speaking, softening under compression is due to persistent microcracking, not due to plastic strains as in the current formulation, which leads to the concept of damage in compression.

6 ACKNOWLEDGEMENTS

E. Hansen and K. Willam would like to thank CASI (Colorado Advanced Software Institute) for partial funding of this research. Travel support for the collaboration through a grant from the US-Spain Commission for Cultural and Scientific Exchange between the University of Colorado and ETSECCPB-UPC, is appreciated. The third author also wishes to acknowledge partial support for this research from MCYT (Madrid) through grant MAT2000-1007, and funding for his Fall/2000 stay at the Univ. of Colorado received from Generalitat de Catalunya (Barcelona).

REFERENCES

- Carol, I. and P. Prat (1995). A multicroack model based on the theory of multisurface plasticity and two fracture energies. In D. Owen and E. Oñate (Eds.), *Computational plasticity, fundamental and applications*, Barcelona. Pineridge Press Limited.
- Carol, I., E. Rizzi, and K. Willam (1994). A unified theory of elastic degradation and damage based on a loading surface. *International Journal of Solids and Structures* 31(20), 2835–2865.
- Carol, I., E. Rizzi, and K. Willam (2001). On the formulation of anisotropic elastic degradation. I: Theory based on a pseudo-logarithmic damage tensor rate, II: Generalized pseudo-rankine model for tensile damage. *International Journal of Solids and Structures* 38(4), 491–546.
- Drucker, D. and W. Prager (1952). Soil mechanics and plastic analysis or limit design. *Quarterly of applied mathematics* 10, 157–165.
- Etse, G. and K. Willam (1994). A fracture energy formulation for inelastic behavior of plain concrete. *ASCE J. Eng. Mech. div.* 120(9), 1983–2011.
- Hansen, E. (2000, December). *A two-surface anisotropic damage/plasticity model for plain concrete*. Ph. D. thesis, University of Colorado at Boulder, Boulder, CO.
- Ortiz, M. (1985). A constitutive theory for the inelastic behavior of concrete. *Mechanics of Materials* 4, 67–93.
- Valanis, K. (1990). A theory of damage in brittle materials. *Engineering fracture mechanics* 36(3), 403–416.